Surface Tension of Liquid Ag–Cu Binary Alloys

Jürgen BRILLO,[1]* Giorgio LAULETTA,[2] Luca VAIANELLA,[2] Elisabetta ARATO,[2] Donatella GIURANNO,[3] Rada NOVAKOVIC[3] and Enrica RICCI[1]

1) Institut für Materialphysik im Weltraum, Deutsches Zentrum für Luft- und Raumfahrt, 51170 Köln, Germany.
2) Dept. of Chemical Eng. (DICCA), University of Genoa, Via dell'Opera pia, 15, 16145 Genoa, Italy.
3) Institute for Energetics and Interphases (CNR-IENI), National Research Council, Via Marini 6, 16149 Genoa, Italy.

Surface tension of liquid Ag–Cu binary alloys has been measured contactlessly using the technique of electromagnetic levitation in combination with the oscillating drop technique. The measurements were performed at temperatures above the melting point of alloys. The surface tension values were obtained from an analysis of the frequency spectra of droplet oscillations recorded with a CMOS-camera at 400 fps.

The alloy samples covered the entire composition range. The surface tension data can be described by linear functions of temperature with negative slopes. The new experimental data were compared to the corresponding theoretical values calculated combining the Butler equation with the ideal and subregular solution models, respectively. The agreement with the experimentally obtained data is excellent for the isothermal surface tension and quite reasonable for their temperature coefficients.

KEY WORDS: Ag–Cu liquid alloys; butler equation; electromagnetic levitation; segregation; surface tension.

1. Introduction

Binary Ag–Cu liquid alloys serve as a model for the study of solidification and growth processes in eutectic materials.[1,2] The phase diagram,[3,4] exhibits an extended solid solubility range on both sides and an eutectic point at the composition of $Ag_{60}Cu_{40}$ with a transition temperature of 1 053 K.

In the liquid state, the Ag–Cu displays ideal mixing behavior with respect to its density.[5] This observation can be associated with a close similarity of the two components, Ag and Cu, which are both in group Ib in the periodic table and, hence, have a similar electronic configuration ([Ar]$3d^{10}4s^1$ for Cu and [Kr]$4d^{10}5s^1$ for Ag).[6]

The Ag–Cu system is also interesting for a number of technical/industrial applications in joining processes. Such applications are brazing, soldering and welding. In particular, ternary Sn–Ag–Cu alloys (SAC) serve as replacement material for the lead containing Sn–Pb alloys conventionally used for soldering electronic compounds.[7–10] Moreover, Ag–Cu alloys are also used in high temperature bonding applications where, at the interface, it comes to the formation of ternary Al–Ag–Cu alloys.[11]

In these examples, nucleation, solidification and growth processes go hand-in-hand with key dynamic processes associated to surface and interfacial properties of a melt.[12] In order to fully understand such processes, precise knowledge of the surface tension is indispensable.

Although Ag–Cu is chemically rather an inert system, there is still the risk of pollution due to chemical reactions if the surface tension is measured using a container-based technique. On the other hand, containerless methods, such as electromagnetic levitation,[13] circumvent this problem. Moreover, and in contrast to container-based techniques, the free surface is the only interface in the system.[14]

In this paper, we show the results of surface tension measurement performed on Ag–Cu alloy melts using electromagnetic levitation as a containerless technique. These were obtained and discussed as functions of temperature and alloy composition.

2. Butler Equation

In a number of previous studies, such as[15–27] it was shown that the surface tension of liquid binary and ternary alloys can be successfully described by the Butler equation[28] which treats the surface as an individual thermodynamic phase being in equilibrium with the bulk.

When i denotes one element of the alloy, (i = Cu, Ag), $\gamma_i(T)$ denote their corresponding surface tensions at temperature T, ^Bx_i, denotes the concentration of element i in the bulk phase, and ^Sx_i the concentration in the surface phase, the Butler equation is given by the following expression for the present case:

$$\gamma_{AgCu}(T) = \gamma_{Ag} + \frac{RT}{S_{Ag}}\ln\left(\frac{^Sx_{Ag}}{^Bx_{Ag}}\right) + \frac{1}{S_{Ag}}\left\{^EG_{Ag}^S(T,{^Sx_{Ag}}) - {^EG_{Ag}^B(T,{^Bx_{Ag}})}\right\}$$

$$= \gamma_{Cu} + \frac{RT}{S_{Cu}}\ln\left(\frac{1-{^Sx_{Ag}}}{1-{^Bx_{Ag}}}\right) + \frac{1}{S_{Cu}}\left\{^EG_{Cu}^S(T,1-{^Sx_{Ag}}) - {^EG_{Cu}^B(T,1-{^Bx_{Ag}})}\right\}$$

.... (1)

Here, R is the universal gas constant, $^EG_i^B$ and $^EG_i^S$ (i = Ag,

Cu) denote the respective partial excess free energies of component i in the bulk and in the surface layer, and S_i is the partial molar surface area of pure liquid i which is estimated from the molar volume of the pure element, V_i, using a value of 1.091 for the geometrical factor.[19,29]

In order to apply the Butler model another assumption becomes important, i.e. the approximation of the surface excess free energy, ${}^E G^S(T, {}^S x_i)$, by:[30]

$$ {}^E G^S(T, {}^S x_i) \approx \xi \cdot {}^E G^B(T, {}^S x_i) \quad \text{.................. (2)} $$

The phenomenological factor ξ accounts in a crude way for the reduced coordination in the surface layer. A constant value of 0.83 was suggested by Tanaka and Iida as a default approximation for liquids with unknown structure.[31] This value is also used in the present calculations.

The excess energy ${}^E G^B$, needed in order to derive the partial excess energies is usually written in the following Redlich-Kister form:[32]

$$ {}^E G^B = {}^B x_{Ag} \, {}^B x_{Cu} \sum_{v=0} ({}^v A + {}^v BT)({}^B x_{Ag} - {}^B x_{Cu})^v \quad \text{.... (3)} $$

In Eq. (3), the coefficients ${}^v A$ and ${}^v B$ do not depend on temperature and concentrations. Details of the solution of the Butler equation are also described in Refs. 15)–19).

All parameters used to solve the Butler equation are listed in **Table 2**. The molar volumes are calculated from the densities which have been taken from Ref. 5). They are represented as linear functions of temperature with the two adjustable parameters, ρ_L being the density at T_L and ρ_T which is the temperature coefficient. The parameters ${}^v A$ and ${}^v B$ needed in Eq. (3) for the calculation of the excess free energy are taken from Witusievicz[33] and listed in **Table 3**.

3. Experimental

Experiments were performed in a standard stainless steel high vacuum chamber filled with 800 mbar He, Ar or a mixture of both after prior evacuation. The purity of the gases was 99.9999 vol.%. The samples having typical diameters of 4 mm were positioned in the centre of a levitation coil. The high frequency inhomogeneous electro-magnetic field induces eddy currents inside the sample so that it can be positioned stably against gravity. Due to ohmic losses of the current the sample is heated and molten. In order to adjust a certain desired temperature, it is cooled in a laminar flow of the He gas. The temperature was measured by a pyrometer focussed at the sample from the side. As the emissivity is generally not known, it is determined from the pyrometer output signal at the known liquidus temperature T_L under the valid assumption that within the operating wavelength range of the pyrometer the emissivity of the specimen material does not change with temperature. The details of this procedure are described in.[5]

In the present work, values for T_L were obtained from the phase diagram reported in,[3] see **Table 1**.

The frequencies of the droplet oscillations serve as a direct measure of the surface tension γ. In ground based electromagnetic levitation, the symmetry of the sample is reduced as compared to a droplet under micro gravity which is almost spherical. This leads to a split up of the $l = 2$ Rayleigh oscillation mode into a set of five frequencies ω_m

Table 1. Parameters T_L, γ_L, and γ_T of each of the investigated alloys. The table also shows the interpolated surface tension at 1 423 K.

Composition	T_L [K]	γ_L [N/m]	γ_T [10^{-4}·N/m/K]	$\gamma(T = 1\,423\,\text{K})$ [N/m]
Cu	1 358	1.334	–2.6	1.317
$Ag_{10}Cu_{90}$	1 284	1.129	–0.70	1.119
$Ag_{20}Cu_{80}$	1 215	1.069	–1.42	1.040
$Ag_{40}Cu_{60}$	1 113	0.989	–0.51	0.970
$Ag_{40}Cu_{60}$	1 113	0.951	–0.30	0.942
$Ag_{60}Cu_{40}$	1 053	0.926	–1.00	0.889
$Ag_{60}Cu_{40}$	1 053	0.911	–0.59	0.889
$Ag_{60}Cu_{40}$	1 053	0.930	–0.23	0.921
Ag	1 234	0.894	–1.91	0.858

Table 2. Parameters entering the Butler equation: Surface tension, γ_L, and density, ρ_L, of the pure components at liquidus, T_L, and their respective temperature coefficients, γ_T and ρ_T. Density data were taken from Brillo.[5]

	Ag	Cu
T_L [K]	1 234	1 358
γ_L [N/m]	0.894	1.334
γ_T [10^{-4}·N/m/K]	–1.91	–2.56
ρ_L [g/cm^3]	9.15	7.90
ρ_L [10^{-4}·g/cm^3/K]	–7.4	–7.6

Table 3. Parameters ${}^v A$ and ${}^v B$ entering the Redlich-Kister equation, Witusievic.[33]

v	${}^v A$ [kJ/mol]	${}^v B$ [10^{-3} kJ/mol/K]
0	14.463	–1.516
1	–0.934	–0.319

with $m = -2, -1, 0, 1, 2$.

These are measured by recording of 4 096 images of the oscillating drop using a C-MOS camera with 400 frames per second (fps). An edge detection and analysis algorithm produces frequency spectra from the time signals, such as the one shown in **Fig. 1**. They are Fourier transforms of the difference and the sum signal of two perpendicular radii. Using symmetry rules[13] the frequencies ω_m, marked by arrows in Fig. 1, can be identified. γ is calculated from these frequencies using the formula of Cummings and Blackburn:[34]

$$ \gamma = \frac{3M}{160\pi} \sum_{m=-2}^{2} \omega_m^2 - 1.9\Omega^2 - 0.3\left(\frac{g}{a}\right)^2 \Omega^{-2} \quad \text{......... (4)} $$

Here M is the mass of the sample, a its radius, and g is the gravitational acceleration. In Eq. (4), the parameter Ω corrects for the magnetic pressure. It is calculated from the three translational frequencies, ω_X, ω_Y, ω_Z corresponding to the horizontal and vertical movements of the center of gravity of the sample: $\Omega^2 = 1/3(\omega_X^2 + \omega_Y^2 + \omega_Z^2)$. From measurements published in[17] the relative error $\Delta\gamma/\gamma$ is estimated to be about 5%.

4. Results

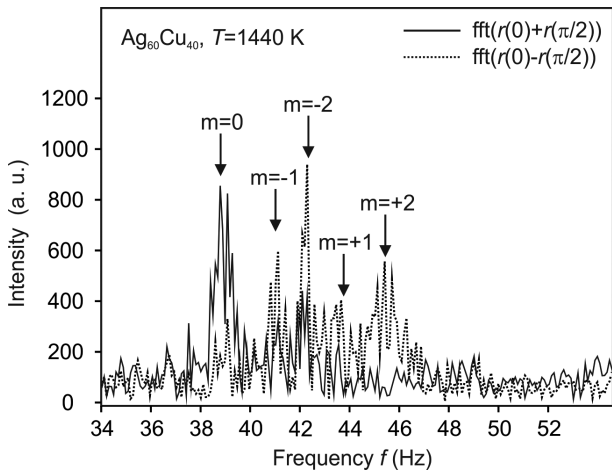The Ag–Cu samples can be levitated and molten. Due to

Fig. 1. Frequency spectra of the surface oscillation of a $Ag_{60}Cu_{40}$ sample at 1 440 K. The solid curve is the Fourier transform of the sum signal of two perpendicular radii and the dotted curve is the Fourier transform of the difference signal.
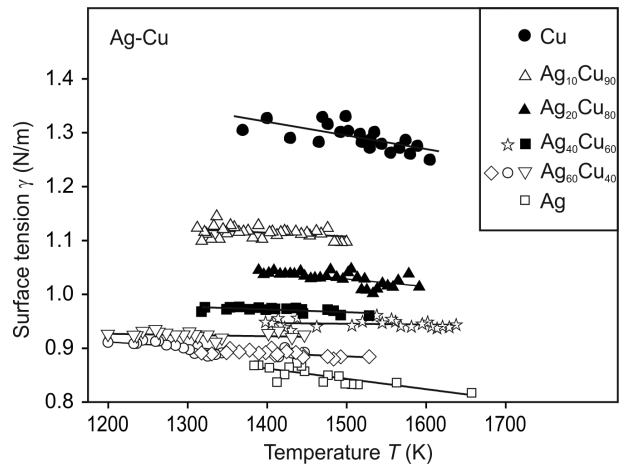

Fig. 2. Measured surface tension γ of liquid Ag–Cu samples versus temperature.

Fig. 3. Isothermal surface tension γ versus silver bulk mole fraction $^{B}x_{Ag}$ at $T = 1\,423$ K (triangles) at $T = 1\,623$ K (circles). The lines correspond to calculations of the Butler equation, Eq. (1), for the ideal (dashed) and the subregular solution model[33] (solid) at 1 423 K and for the subregular solution model[33] at 1 623 K (dash-dotted).

Fig. 4. Temperature coefficient γ_T versus silver bulk mole fraction $^{B}x_{Ag}$. The solid line was calculated by the Butler equation, Eq. (1), as described in the text and by using the subregular solution model.[33]

its high vapour pressure, the maximum temperature was limited to $T \leq T_L + 300$ K. Mass loss due to evaporation did not exceed 1% of the original mass. On the other side, an undercooling was not observed.

Measured surface tension values for pure liquid Ag and Cu, as well as for the investigated binary alloys, $Ag_{60}Cu_{40}$, $Ag_{40}Cu_{60}$, $Ag_{20}gCu_{80}$, and $Ag_{10}Cu_{90}$ as function of temperature are shown in **Fig. 2**. For some of these compositions, such as $Ag_{40}Cu_{60}$ and $Ag_{60}Cu_{40}$, the measurements were repeated.

In Fig. 2, the new surface tension data measured values are represented as a linear function of temperature T by straight lines having negative slopes for each composition. Thus, the following linear law can be fitted to the data:

$$\gamma = \gamma_L + \gamma_T(T - T_L) \qquad \text{.......................... (5)}$$

where γ_L is the surface tension at liquidus temperature T_L and γ_T is the temperature coefficient $\partial\gamma/\partial T$. The results of these fits are shown in Fig. 2 as solid straight lines. For each alloy sample, the fitted parameters, Eq. (5), γ_L and γ_T, are listed in Table 1.

In order to study the concentration dependence of the surface tension, γ was interpolated by Eq. (5) to $T = 1\,423$ K. This temperature was chosen, because it lies in the middle of the temperature ranges of all investigated samples. The results of these interpolations, $\gamma(T = 1\,423$ K$)$, are listed in Table 1 as well. They are plotted in **Fig. 3** versus the silver bulk mole fraction $^{B}x_{Ag}$. As can be seen from this figure, the largest surface tension is obtained for pure copper. At 1 423 K, γ equals 1.317 N/m. When the bulk silver mole fraction $^{B}x_{Ag}$ is increased to 0.1 the surface tension γ decays quickly down to approximately 1.1 N/m. This decay continues upon further increase of $^{B}x_{Ag}$ but with diminished speed. For $^{B}x_{Ag} > 0.5$, $\gamma < 1.0$ N/m until finally the value of pure silver, $\gamma = 0.858$ N/m, is reached (see also Table 1).

In **Fig. 4**, the temperature coefficient γ_T is plotted versus $^{B}x_{Ag}$. The scatter of these data is obviously larger than that in Fig. 3. This has to do with the fact that, generally, γ_T is influenced by different sources of error, such as evaporation or strong sample rotations which directly or indirectly depend on temperature. Therefore an absolute uncertainty of
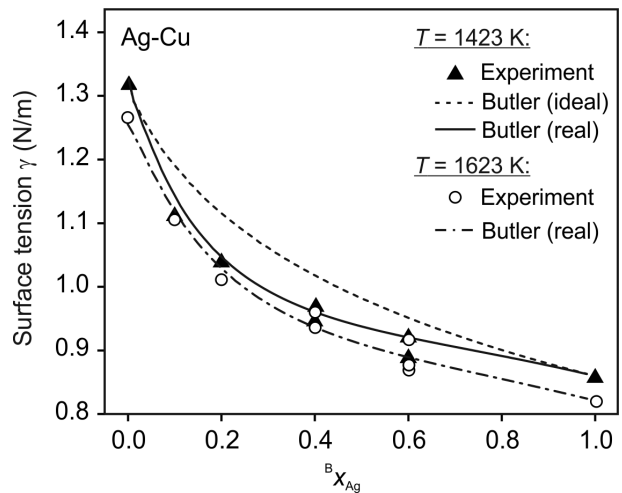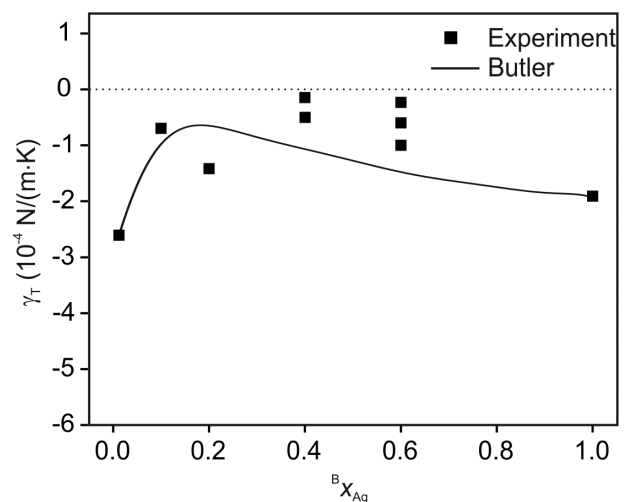
γ_T can be estimated as ± 50%.

Starting on the left hand side (Fig. 4), γ_T strongly increases from a value of $-2.56 \cdot 10^{-4}$ N/m/K, corresponding to pure liquid copper, up to approximately $-1.0 \cdot 10^{-4}$ N/m/K when $^B x_{Ag}$ is increased to only 0.1. Upon further increase of $^B x_{Ag}$, γ_T scatters around values of roughly $5 \cdot 10^{-5}$ N/m/K. A weak and broad maximum (or even a plateau) may be identified around $^B x_{Ag} = 0.5$ before γ_T relaxes back to a value of $-1.9 \cdot 10^{-4}$ N/m/K for pure liquid Ag.

5. Discussion

The measured values of γ_L and γ_T for the pure elements Ag and Cu, respectively together with corresponding results from various literature sources[15,17,35-45] are listed in **Tables 4** and **5**. Concerning pure silver γ_L varies around 0.91 (± 0.01) N/m (Table 4) if the freak value, $\gamma_L = 0.966$ N/m reported by Hibiya[35] is ignored. In the present work γ_L is obtained for pure silver as 0.894 N/m. This value is lower than all other parameters, but still within the margins. The same holds for γ_T which is determined as $-1.91 \cdot 10^{-4}$ N/m/K. The average value is $\gamma_T = -2.1$ (± 0.1) 10^{-4} N/m/K, given in Table 4.

In Table 5, the listed values γ_L of pure copper scatters around 1.31 (± 0.02) N/m. This fits well to the value of 1.334 N/m for γ_L obtained in the present work. The same was found for the temperature coefficient, γ_T, which scatters around a value of $-2.4 \, 10^{-4}$ N/m/K, given in Table 5. $\gamma_T = -2.56 \cdot 10^{-4}$ N/m/K is within the margin of approximately ± $0.25 \cdot 10^{-4}$ N/m/K.

Table 4. Compilation of surface tension values, γ_L and γ_T, for liquid silver. (Method keys: EML = electromagnetic levitation, SD = variant of the sessile drop method, R = review).

γ_L (N·m^{-1})	γ_T (10^{-4} N·m^{-1}K^{-1})	Author, Reference	Method
0.966	−2.5	Hibiya[35]	EML
0.91	−1.8	Egry[36]	EML
0.925	−2.1	Mills[37], Keene[38]	R
0.916	−2.28	Lee[39]	SD
0.914	−1.5	Novakovic[40]	SD
0.894	−1.9	this work	EML

Table 5. Compilation of surface tension values, γ_L and γ_T, for liquid copper. (Method keys: EML = electromagnetic levitation, SD = variant of the sessile drop method, R = review).

γ_L (N·m^{-1})	γ_T (10^{-4} N·m^{-1}K^{-1})	Author, Reference	Method
1.33	−2.3	Mills[41]	R
1.30	−2.86	Brooks[42]	EML
1.29	−2.3	Brillo[15]	EML
1.30	−2.5	Shen[43]	SD
1.29	−1.6	Laty[44]	SD
1.30	−2.64	Schmitz[17]	EML
1.34	−1.8	Novakovic[40]	SD
1.33	−2.3	Amore[45]	EML
1.334	−2.56	present work	EML

The experimental data are compared with the corresponding values obtained by the Butler equation for the ideal and the sub-regular solution models at 1 423 K (Fig. 4). In the ideal solution model the Butler equation is solved for $^E G = 0$. As shown in Fig. 4 the course of the experimental data is qualitatively correctly predicted, *i.e.* that the calculation reproduces that the data collapse on a convex curve. However, the ideal solution model systematically overestimates the experimental data. Depending on composition, the deviation reaches up to 10%.

A much better agreement between the experimental data and the calculated values is obtained if $^E G$ is calculated from the regular solution model, *i.e.* from Eq. (3) with $^E G$ taken from Witusievic.[33] In Fig. 4, the calculation reproduces the experimental data within their scatter and the agreement is excellent.

In order to compare the Butler equation with the measured temperature coefficients, γ_T, Eq. (1) is calculated for two different temperatures, $T_1 = 1 423$ K and $T_2 = 1 523$ K. Then γ_T is estimated from these runs as $\gamma_T \approx (\gamma(T_1) - \gamma(T_2)) / (T_1 - T_2)$. The result is shown in Fig. 4. Qualitatively, the course of the experimental data with their steep increase on the copper rich side and the plateau in the middle is reproduced. The overall agreement between the experimental data and the calculation can be judged as reasonable, although the calculation slightly underestimates the experiment for $0.4 \leq \, ^B x_{Ag} \leq 0.6$. Relative to the surface tension, this deviation is in the order of less than $<10^{-5}$. An uncertainty of γ_T being in the same order as γ_T itself should have a negligible effect on the prediction of γ. This is demonstrated in Fig. 3 where the Butler equation is compared to the experimentally obtained surface tensions at 1 623 K. As visible, the agreement between calculation and experiment is very good at this temperature as well.

In addition to the surface tension and its temperature coefficient, Eq. (1) also provides information on the composition in the surface layer, see Novakovic.[40] The surface mole fraction of silver, $^S x_{Ag}$ vs the bulk mole fraction, $^B x_{Ag}$ for $T = 1 423$ K is plotted in **Fig. 5**. Obviously, silver is
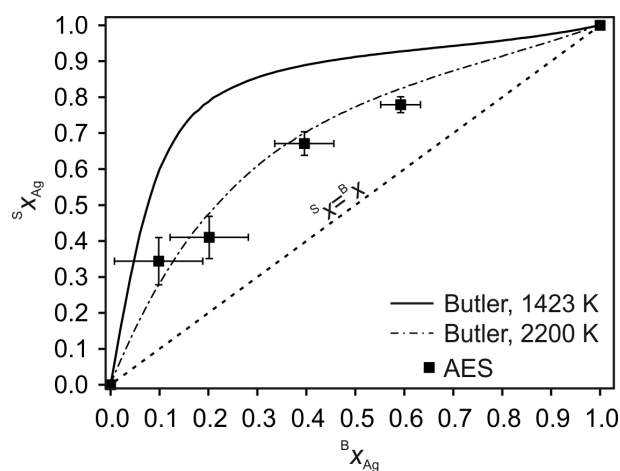

Fig. 5. Calculated surface silver mole fraction, $^S x_{Ag}$, versus the bulk mole fraction $^B x_{Ag}$ at 1 423 K (solid line) and at 2 200 K (dash-dotted line). The symbols correspond to experimental data obtained by AES analysis.[46] The dashed line marks the equality of $^B x_{Ag}$ and $^S x_{Ag}$ and was drawn in order to aid the eye.

enriched in the surface layer as $^Sx_{Ag} > {}^Bx_{Ag}$. $^Sx_{Ag}$ strongly increases to $^Sx_{Ag} \approx 0.8$ when the corresponding bulk mole fraction $^Bx_{Ag}$ is increased to 0.2. Upon further increase of $^Bx_{Ag}$ the slope of $^Sx_{Ag}$ has drastically become smaller and $^Sx_{Ag}$ finally reaches unity for $^Bx_{Ag} = 1$.

It is justified to ask whether or not the calculated surface compositions are reliable. In general, experimental data for a validation are difficult to obtain. However, in the case of Ag–Cu liquid alloys, Williams and Norris[46] have performed Auger electron spectroscopy (AES) measurements on surfaces of Ag–Cu melts. In their experiments, they also determined $^Sx_{Ag}$. Unfortunately, nothing was reported about the temperature at which these experiments were carried out. This circumstance makes it difficult to compare their results with our calculation. Nevertheless, their results are plotted in Fig. 5 as well.

As visible, the AES data exhibit qualitatively the same trend as our calculation. Namely, they confirm that silver is segregating at the surface. However, the calculation overestimates the experimental data of [32] by nearly 100%. Hence, the quantitative agreement between the Butler equation and the AES data is not significant. Of course, the results obtained from the Butler equation can strongly depend on the used input data, for instance on the thermodynamic assessment used, or the fact, that the temperature, for which the calculation was carried out, 1 423 K, is most likely not the same as the one at which the AES experiments have been performed. In order to discuss the effect of the different temperatures, T was adjusted in the Butler equation, Eq. (1), such that the AES data could be reproduced, see Fig. 5. However, this was possible only for $T = 2 200$ K which is rather unrealistic. If their temperature was lower than 1 423 K segregation would have become even more pronounced in their results.

One can also identify the following as potential reason for the discrepancy in Fig. 5: It is a fact that, although AES is regarded as surface sensitive,[47] it will always average over the top few monolayers, depending on the penetration depth of the secondary electrons with their element specific kinetic energies. This effect will certainly decrease the experimental results obtained for $^Sx_{Ag}$, as segregation is less pronounced in sub surface layers.

6. Summary

Surface tension data of liquid Ag–Cu binary alloys have been measured in a containerless way by the oscillating drop technique. The measurements were performed on the alloy samples covering the entire composition range and for temperatures at and up to 300 K above the melting point. It was found that the surface tensions can be described by linear functions of temperature with negative slopes. The new experimental results of pure silver and copper were in good agreement with corresponding literature data.

Calculations based on the Butler equation using the ideal- and subregular solution approximation exhibited excellent agreement for the isothermal surface tension and quite reasonable agreement for their temperature coefficients. Comparison of the predicted surface composition with published results obtained from Auger analysis was successful only from a qualitative point of view.

Further research will be focussed on the influence of oxygen on the surface tension in this system.

REFERENCES

1) D. J. S. Cooksey and A. Hellawell: *J. Inst. Met.*, **95** (1967), 183.
2) J. De Wilde, L. Froyen and S. Rex: *Scr. Mater.*, **51** (2004), 533.
3) T. B. Massalski: Binary Alloy Phase Diagram, American Society for Metals, Materials Park, OH, (1986).
4) T. Massalski and J. Perepezko: *Z. Metallkd.*, **64** (1973), 176.
5) J. Brillo, I. Egry and I. Ho: *Int. J. Thermophys.*, **27** (2006), 494.
6) http://www.webelements.com/, (accessed 2014-2-1).
7) R. Novakovic, T. Lanata, S. Delsante and G. Borzone: *Mater. Chem. Phys.*, **137** (2012), 458.
8) V. Sklyarchuk, Y. Plevachuk, I. Kaban and R. Novakovic: *J. Min. Met. Sect.-B-Metall.*, **48** (2012), 443.
9) S. Amore, E. Ricci, T. Lanata and R. Novakovic: *J. Alloys Compd.*, **452** (2008), 161.
10) R. Novakovic, E. Ricci, D. Giuranno, T. Lanata and S. Amore: *Calphad*, **33** (2009), 69.
11) P. Gupta, R. Doraiswami and R. Tumala: *Electron Comp. Technol.*, **1** (2004), 68.
12) A. Genau and L. Ratke: *Int. J. Mater. Res.*, **103** (2012), 469.
13) J. Brillo, G. Lohöfer, F. Schmidt-Hohagen, S. Schneider and I. Egry: *Int. J. Mater. Prod. Technol.*, **26** (2006), 247.
14) I. Egry, E. Ricci, R. Novakovic and S. Ozawa: *Adv. Coll. Interfac. Sci.*, **159** (2010), 198.
15) J. Brillo and I. Egry: *J. Mater. Sci.*, **40** (2005), 2213.
16) J. Brillo, Y. Plevachuk and I. Egry: *J. Mater. Sci.*, **45** (2010), 5150.
17) J. Schmitz, J. Brillo, I. Egry and R. Schmid-Fetzer: *Int. J. Mater. Res.*, **100** (2009), 1529.
18) J. Brillo, D. Chatain and I. Egry: *Int. J. Mater. Res.*, **100** (2009), 53.
19) J. Brillo, I. Egry and T. Matsushita: *Z. Metallkd.*, **97** (2006), 28.
20) T. Tanaka and T. Iida: *Steel Res.*, **65** (1994), 21.
21) K. Monma and H. Suto: *J. Jpn. Inst. Met.*, **25** (1961), 143.
22) K. Yeum, R. Speiser and D. Poirier: *Metall. Trans.*, **B20** (1989), 693.
23) H. Lee, M. Frohberg and J. Haira: *Steel Res.*, **64** (1993), 191.
24) Z. Moser, W. Gasior and J. Pstrus: *J. Phase Equilibria*, **22** (2001), 254.
25) R. Picha, J. Vrestal and A. Kroupa: *Calphad*, **28** (2004), 141.
26) X. Liu, T. Yamaki, I. Ohnuma, R. Kainuma and K. Ishida: *Mater. Trans.*, **45** (2004), 637.
27) L. Yan, S. Zheng, G. Ding, G. Xu and Z. Oiao: *Calphad*, **31** (2007), 112.
28) J. Butler: *Proc. Roy. Soc.*, **A135** (1935), 135.
29) G. Kaptay: *Proc. Microcad, Section: Mater. Sci., Univ. of Miskolc*, **45** (2002).
30) T. P. Hoar and D. A. Melford: *Trans. Farad. Soc.*, **33** (1957), 315.
31) T. Tanaka, K. Hack, T. Iida and S. Hara: *Z. Metallkd.*, **87** (1996), 380.
32) C. Lüdecke C and D. Lüdecke: Thermodynamik, Springer, Heidelberg, (2000).
33) V. T. Witusiewicz, U. Hecht, S. G. Fries and S. Rex: *J. Alloys Compd.*, **385** (2004), 133.
34) D. L. Cummings and D. A. Blackburn: *J. Fluid. Mech.*, **224** (1991), 395.
35) T. Hibiya, K. Morohoshi and S. Ozawa: *J. Mater. Sci.*, **45** (2010), 1986.
36) I. Egry and S. Sauerland: *High Temp.- High Press.*, **26** (1994), 217.
37) K. C. Mills and Y. C. Su: *Int. Mater. Rev.*, **51** (2006), 329.
38) B. Keene: *Int. Mater. Rev.*, **38** (1993), 157.
39) J. Lee, W. Shimoda and T. Tanaka: *Mater. Trans.*, **45** (2004), 2864.
40) R. Novakovic, E. Ricci, D. Giuranno and A. Passerone: *Surf. Sci.*, **576** (2005), 175.
41) K. C. Mills: Recommended Values of Thermophysical Properties for Selected Commercial Alloys, Woodhead Publishing Ltd., Cambridge, UK, (2002).
42) R. F. Brooks, K. C. Mills, I. Egry, D. Grant, S. Seetharaman and B. Vinet: NPL Report, CMMT(D), The National Physical Laboratory, UK, (1998), 136.
43) P. Shen, H. Fujii, T. Matsumoto and K. Nogi: *J. Mater. Sci.*, **40** (2005), 2329.
44) P. Laty, J. C. Joud and P. Desre: *Surf. Sci.*, **69** (1977), 508.
45) S. Amore, J. Brillo, I. Egry and R. Novakovic: *Appl. Surf. Sci.*, **257** (2011), 7739.
46) G. P. Williams and C. Norris: *Philos. Mag.*, **34** (1976), 851.
47) D. Briggs and M. P. Seah: Practical Surface Analysis, 2nd ed., Vol. 1, Wiley, New York, (1983).